タイトル	Changes in Bruch's Membrane Opening-Minimum Rim Width after Reduction of Intraocular Pressure in Eyes with Open-Angle Glaucoma
作成者（著者）	Takumi, Tetsuro / Enomoto, Nobuko / Ishida, Kyoko / Tomita, Goji
公開者	The Medical Society of Toho University
発行日	2019.12.01
ISSN	21891990
掲載情報	Toho Journal of Medicine. 5(4). p.161-172.
資料種別	学術雑誌論文
内容記述	Original Article
著者版フラグ	publisher
JaLCDOI	info:doi/10.14994/tohojmed.2019-008
メタデータのＵＲＬ	https://mylibrary.toho-u.ac.jp/webopac/TD35034279

Original Article

Changes in Bruch's Membrane Opening-Minimum Rim Width after Reduction of Intraocular Pressure in Eyes with Open-Angle Glaucoma

Tetsuro Takumi[1,2]* Nobuko Enomoto[2] Kyoko Ishida[2]
and Goji Tomita[2]

[1] Department of Ophthalmology, Toho University Graduate School of Medicine, Tokyo, Japan
[2] Department of Ophthalmology, Toho University Ohashi Medical Center, Tokyo, Japan

ABSTRACT

Introduction: Bruch's membrane opening-minimum rim width (BMO-MRW) is measured perpendicular to the neural tissue axis and considers the variable trajectory of axons over the point of measurement, similar to the measurement strategies used for circumpapillary retinal nerve fiber layer thickness (c-RNFLT). However, changes in BMO-MRW in relation to those in c-RNFLT with intraocular pressure (IOP) reduction remain unclear. This study evaluated changes in BMO-MRW and their relationship to changes in the optic nerve head cup size and c-RNFLT in patients with open-angle glaucoma post-trabeculectomy (TLE).

Methods: Thirty-one eyes of 31 patients were enrolled. All patients underwent fundus imaging with spectral domain-optical coherence tomography before and three months after TLE. We measured BMO-MRW and c-RNFLT and evaluated the cup size by calculating the cup profile area using the ImageJ program.

Results: Reduction of IOP led to a significant increase in BMO-MRW and a significant decrease in cup size. Changes in the BMO-MRW of the whole disc and the temporal superior segments correlated significantly with the change in IOP. In multiple regression analysis, there was a significant relationship between the changes in cup size and axial length (but not the change in IOP) and the change in BMO-MRW. Although c-RNFLT did not increase significantly post-TLE, the mean deviation of the visual field at baseline, cup size at baseline, and change in cup size were considered to contribute to the change in c-RNFLT.

Conclusions: BMO-MRW increased after adequate TLE-induced reduction of IOP. The increase in BMO-MRW was related to the cup size and reduction in axial length.

Toho J Med 5 (4): 161–172, 2019

KEYWORDS: glaucoma, spectral-domain optical coherence tomography, Bruch's membrane opening

Introduction

The structural reversibility of optic disc cupping after intraocular pressure (IOP) reduction is well documented. A reduction in cup size and an increase in the retinal nerve fiber layer thickness (RNFLT) are both reported.[1,2] Reversal of cupping reportedly occurs more often in patients treated surgically than in those treated medically.[1–4]

*Corresponding Author: Tetsuro Takumi, 2-22-36 Ohashi, Meguro, Tokyo 153-8515, Japan, tel: +81–3–3468–1251
e-mail: mokofusyu@gmail.com
DOI: 10.14994/tohojmed.2019-008

Received May 1, 2019: Accepted July 18, 2019
Toho Journal of Medicine 5 (4), Dec. 1, 2019.
ISSN 2189–1990, CODEN: TJMOA2

Most patients with a 40% lower IOP after glaucoma surgery show improved optic nerve morphology as measured by scanning laser tomography.[5, 6] The amount of improvement correlates highly with the percent reduction in IOP.[6, 7] Reduction of the cup size is accompanied by apparent thickening of the neuroretinal rim[6–8] and depends on the anterior repositioning of a posteriorly displaced lamina cribrosa, resulting from changes in the translaminar pressure gradient.[9]

Recent studies have demonstrated that spectral-domain optical coherence tomography (SD-OCT) allows for anatomically accurate quantification of the disc margin.[10] The Bruch's membrane opening (BMO), i.e., the termination of Bruch's membrane, is an accurate anatomic boundary of the neuroretinal rim tissue. Gardiner et al.[11] demonstrated that minimum rim-width measurements from BMO, the shortest distance from the BMO to the inner limiting membrane (BMO-MRW), are significantly better correlated with both RNFLT and the visual field mean deviation (MD) than rim measurements within the BMO plane or hose based on the clinical disc margin. Chauhan et al.[12] also reported that BMO-MRW has a better diagnostic performance for open-angle glaucoma than current disc margin measurements. However, how the BMO-MRW changes with changes in IOP, particularly IOP reduction, is not clear. Gieztelt et al.[13] recently assessed the impact of trabeculectomy (TLE) on BMO-MRW and reported that, although the increase in BMO-MRW six months after surgery correlated with the reduction in IOP, the RNFLT remained stable between baseline and follow-up at 3, 6, and 12 months and showed a moderate loss after 18 months of follow-up. They concluded that the structural reversal of disc cupping influences BMO-MRW for more than one year after glaucoma surgery, leading to a significant increase in the morphometric parameters. The amount of improvement in the morphometric parameters correlated highly with the relative reduction in IOP, but the authors did not measure the actual amount of cup reversal. Therefore, how the amount of cup changes relates to the changes in BMO-MRW after IOP reduction remains unclear. Furthermore, because BMO-MRW is measured perpendicular to the axis of the neural tissue, it takes into account the variable trajectory of axons over the point of measurement, similar to the current strategies used to measure peripapillary RNFLT.[14] The relationship between the magnitude of change in BMO-MRW, with reduction of IOP, and the magnitude of change in peripapillary RNFLT is also not fully understood.

The purpose of this study was to investigate the relationship between cup reversal and changes in the BMO-MRW and peripapillary RNFLT after reduction of IOP by TLE in eyes with open-angle glaucoma. We also sought to identify factors contributing to the changes in BMO-MRW and RNFLT.

Methods

Subject recruitment

This prospective observational study was approved by the Ethics Committee of Toho University Ohashi Medical Center (H15-85) and adhered to the tenets of the Declaration of Helsinki. Written informed consent was obtained from all patients before inclusion in the study.

The inclusion criteria were (1) a clinical diagnosis of open-angle glaucoma with documented progressive optic disc change and/or visual field damage compatible with glaucoma, (2) best-corrected visual acuity ≥0.6 decimals in the study eye, and (3) refraction within ± 6.00 diopters (D) sphere and ± 3.00 D astigmatism, and (4) at least 20% IOP reduction at the time of postoperative evaluation.

A glaucomatous visual field change was defined as (1) outside normal limits on the glaucoma hemifield test or (2) three abnormal points with P<5% probability of being normal, 1 with P<1% by pattern deviation, or (3) pattern standard deviation of 5% if the visual field was otherwise normal, confirmed on two consecutive tests. A visual field measurement was considered reliable when false-positive/negative results were <25% and fixation losses were < 20%.

The exclusion criteria were (1) concomitant ocular disease and (2) systemic medication known to affect the visual field. Eyes with an axial length ≥26 mm or secondary glaucoma were also excluded, as were eyes for which a good-quality image (i.e., a quality score >20) could not be obtained. If both of a patient's eyes were eligible for the study, one eye was randomly selected for inclusion.

TLE was performed when one or both of the following indications was present: (1) documented and confirmed visual field and/or optic disc progression and (2) IOP considered clinically too high for the level of glaucomatous damage. Patients were scheduled for TLE at the referral practices of two of the authors (GT and KI). Laser suture lysis, bleb needling revision, subconjunctival injection of mitomycin C, and topical ocular hypotensive medications were used postoperatively, at the discretion of the treating surgeon, as clinically indicated.

Clinical examination

All participants underwent the following examinations one day before surgery and three months postoperatively: (1) measurement of visual acuity; (2) refraction using an autorefractometer (RK-5; Canon, Tokyo, Japan); (3) slit-lamp biomicroscopy; (4) Goldmann applanation tonometry; (5) darkroom four-mirror gonioscopy (Ocular Instruments, Bellevue, WA); (6) standard automated perimetry (SAP; SITA-Standard 30-2 program; Humphrey Field Analyzer II-750i; Carl Zeiss Meditec, Dublin, CA); (7) measurement of axial length (IOL Master, Carl Zeiss Meditec); and (8) SD-OCT (Spectralis, Heidelberg Engineering, Heidelberg, Germany) imaging after pupil dilation with 0.4% tropicamide (Midrin-M, Santen Pharmaceutical Co. Ltd., Osaka, Japan).

OCT imaging

Spectral-domain OCT imaging was performed using the Glaucoma Module Premium Edition for Spectralis SD-OCT. For BMO-MRW, a radial scanning pattern centered on the optic nerve head (ONH) was used (24 high-resolution 158 radial scans, each averaged from 30 B-scans with 768 A-scans per B scan acquired with a scanning speed of 40,000 A-scans per second). The BMO position was defined as the end-point of Bruch's membrane layer on either side of the ONH. The inner limiting membrane was delineated automatically by the Spectralis software. We automatically obtained the mean BMO-MRW for the whole disc (global) and six segments (temporal, temporal superior, temporal inferior, nasal, nasal superior, and nasal inferior) from the Spectralis software.

Circumpapillary (c-) RNFLT was also measured using the circular scan protocol of the Spectralis OCT system. The scan comprised 768 A-scans, each representing the mean of 100 individual scans, which were obtained with scan circles subtending 12° and diameters measuring 3.5 mm centered on the BMO center to measure c-RNFLT. Measurements of axial length and corneal curvature were entered into the instrument's software to ensure accurate scaling of all measurements.

The mean c-RNFLT for the whole circular scan (global) and six segments (temporal, temporal superior, temporal inferior, nasal, nasal superior, and nasal inferior) were obtained in a manner similar to that used to acquire the BMO-MRW measurements.

The preoperative images were acquired on the day before surgery and follow-up images were acquired three months after surgery at the same locations as those imaged preoperatively. Follow-up scans were obtained using a built-in automated realignment procedure (referred to as the "follow-up examination" in the system documentation).

The quality of the SD-OCT image was assessed prior to analysis, and images that were of insufficient quality (quality index <25 dB for SD-OCT, as suggested by the manufacturer for image quality assurance) were excluded.

Image processing

The two best corresponding of the 24 preoperative and postoperative radial scans, one passing from temporal-superior to nasal-inferior of the ONH and the other passing from temporal-inferior to nasal-superior of the ONH, in which the surfaces of the prelaminar tissue and BMO were clearly visible, were selected (Fig. 1). We used these radial scans for cup size analysis with a personal computer system (Photoshop CS3, Adobe Corporation, San Jose, CA; ImageJ, National Institutes of Health, Bethesda, MD). A line joining the BMO was used as a reference line for the preoperative and postoperative images. The surrounding area, comprising the pre-laminar tissue surface and reference line, was then measured as "cup size (μm^2)" (Fig. 2). The measurements were converted to square micrometers using the scale bar in the imported images. All delineations and measurements were performed by one observer (TT).

To evaluate the intraobserver reproducibility of the cup size measurements, the same datasets were measured in duplicate, and the intraclass correlation coefficient and coefficient of variation were calculated. According to Fleiss, intraclass correlation coefficients $\geq$0.75, between 0.40 and 0.75, and $\leq$0.4 are considered excellent, moderate, and poor, respectively.[15] We used the average cup size of the temporal-superior to nasal-inferior scan and the temporal-inferior to nasal-superior scan for further analyses.

Statistical analysis

Unless otherwise noted, measurements are shown as the mean ± standard deviation. The Wilcoxon's signed-rank test was used to analyze the differences in IOP, BMO-MRW, c-RNFLT, cup size, axial length, and MD of the visual field test. Differences between groups were analyzed using the Mann-Whitney *U* test or Kruskal-Wallis one-way analysis of variance. Spearman's rank correlation coefficient was used to evaluate the relationship between percent changes [(post-surgery − pre-surgery)/pre-surgery) × 100 (%)] in the factors. Multiple regression analyses were used to determine the factors related to the changes in BMO-MRW and c-RNFLT. All statistical analy-

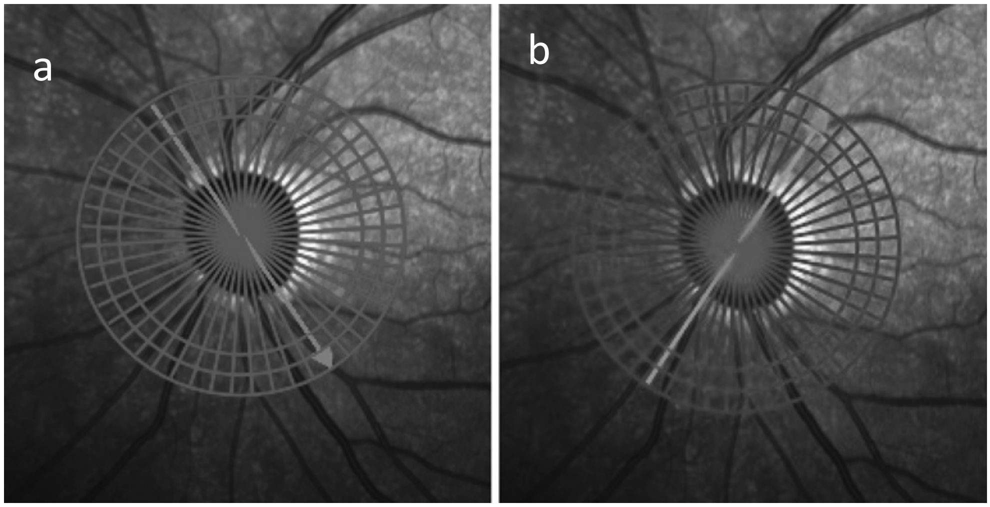

Fig. 1 A representative image of the optic nerve head preoperatively. Among 24 radial scans, the 2 best corresponding scans were selected, one passing from temporal-superior to nasal-inferior of the optic nerve head (ONH) (a) and the other passing from temporal-inferior to nasal-superior of the ONH (b), both preoperatively and postoperatively, in which the surface of the pre-laminar tissue and Bruch's membrane opening were clearly visible.

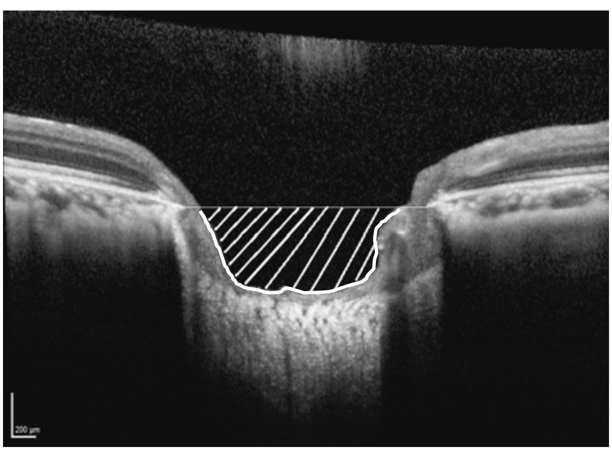

Fig. 2 A line joining the Bruch's membrane opening was used as a reference line. The surrounding area (the yellow shaded area), demarcated by the pre-laminar tissue surface and reference line, was then measured as "cup size (μm^2)".

Table 1 Patient characteristics

Variables		[Range]
Sex		
Male	13 (41.9%)	
Female	18 (58.1%)	
Diagnosis		
POAG	21 (67.7%)	
NTG	6 (19.4%)	
XFG	4 (12.9%)	
Age (years)	69.5 ± 9.8	[48-89]
Axial Length (mm)	24.4 ± 0.8	[23.1-25.96]
IOP (mmHg)	21.8 ± 6.9	[13-35]
Spherical Equivalent (D)	− 1.7 ± 2.0	[− 5.5- + 2.3]
Visual Field MD (dB)	− 14.7 ± 7.1	[− 27.6- − 1.2]

Continuous variables are expressed as N (percentage), mean ± SD, POAG: Primary open angle glaucoma, NTG: Normal tension glaucoma, XFG: Exfoliation glaucoma, IOP: Intraocular pressure, MD: Mean deviation

ses were performed using SPSS for Windows software (version 19; IBM Corp., Armonk, NY). P-values $<$0.05 were considered statistically significant.

Results

Ninety-four of 212 eyes in 210 patients with open-angle glaucoma who underwent TLE in one eye or both eyes between May 12, 2015 and June 5, 2018 and fulfilled the inclusion criteria for refraction and astigmatism were enrolled in the study. Four of these 94 eyes underwent additional glaucoma surgery within three months, one developed a postoperative infection, 26 did not show an IOP reduction $>$20%, and 24 did not have good-quality OCT images or could not undergo OCT imaging; these eyes were excluded from the study. Eight further eyes with an axial length $\geq$26 mm were also excluded. Finally, 31 eyes (31 patients; 13 men, 18 women) were included in the analysis. Table 1 summarizes the baseline characteristics of the subjects. Twenty-one eyes had primary open-angle glaucoma, six had normal-tension glaucoma, and four had exfo-

Table 2 Differences of parameters in pre- and post-surgery.

	Pre-surgery	Post-surgery	P value
IOP (mmHg)	21.8 ± 6.9	12.0 ± 3.8	**<0.001**
Axial length (mm)	24.5 ± 0.8	24.4 ± 0.8	**<0.001**
MD (dB)	− 14.7 ± 7.1	− 15.4 ± 7.5	0.179
BMO Area (μm^2)	2.2 ± 0.5	2.1 ± 0.5	0.383
BMO-MRW (μm)			
Global	133.9 ± 52.1	142.3 ± 53.0	**<0.001**
Temporal	104.8 ± 48.0	107.8 ± 41.7	**0.010**
Temporal Superior	110.8 ± 77.8	119.1 ± 82.1	**0.004**
Temporal Inferior	104.4 ± 66.3	111.0 ± 66.2	**0.008**
Nasal	162.3 ± 63.3	175.7 ± 68.6	**0.004**
Nasal Superior	153.6 ± 77.7	163.6 ± 73.4	**0.002**
Nasal Inferior	154.1 ± 73.1	161.1 ± 75.2	**0.019**
c-RNFLT (μm)			
Global	54.1 ± 13.6	55.1 ± 13.6	0.086
Temporal	45.8 ± 16.4	47.0 ± 16.6	0.080
Temporal Superior	62.3 ± 24.6	63.5 ± 24.9	0.229
Temporal Inferior	53.6 ± 34.3	54.9 ± 34.6	**0.035**
Nasal	52.4 ± 18.4	52.8 ± 19.0	0.694
Nasal Superior	66.3 ± 21.7	67.4 ± 20.2	0.161
Nasal Inferior	58.2 ± 23.8	59.2 ± 24.5	0.417
Cup Size (μm^2)	596907.5 ± 299787.4	509644.4 ± 264137.5	**<0.001**

Continuous variables are expressed as mean ± SD, IOP: Intraocular pressure, MD: Mean deviation, BMO-Area: Bruch's membrane opening area, BMO-MRW: Bruch's membrane opening minimum rim width, c-RNFLT: Circum-papillary retinal nerve fiber layer thickness.
Statistically significant differences for the parameters of pre-surgery and after post-surgery ($P<0.05$) by Wilcoxon's signed rank test are indicated in bold.

liation glaucoma.

After three months, the IOP decreased significantly from 21.8 ± 6.9 mmHg to 12.0 ± 3.8 mmHg ($p<0.001$). Two eyes had low IOP (6 mmHg), but none had complications caused by hypotony, such as a shallow anterior chamber or choroidal detachment, over the clinical course. There was a significant decrease in axial length from 24.5 ± 0.8 mm to 24.4 ± 0.8 mm ($p<0.001$). There was no significant improvement in visual field MD (−14.7 ± 7.1 dB preoperatively and −15.4 ± 7.5 dB postoperatively; p= 0.179; Table 2).

After surgery, BMO-MRW increased significantly in the global and all other segments; the c-RNFLT did not increase significantly except in the temporal inferior segment (Table 2).

The cup size decreased significantly (Table 2). The intraobserver reproducibility of measurements of cup size was 0.999 (preoperatively) and 0.999 (postoperatively) for the temporal-superior to nasal-inferior scan and 0.970 (preoperatively) and 0.996 (postoperatively) for the temporal-inferior to nasal-superior scan. Fig. 3, 4 show representative images of the changes in cup size and BMO-MRW in a glaucomatous eye with middle-stage visual field loss (MD −8.14 dB). The IOP was reduced from 31 mmHg to 11 mmHg. The cup profile before surgery (Fig. 3a) was markedly reduced by three months after surgery (Fig. 3b), mainly because of anterior displacement of the bottom of the cup. BMO-MRW before surgery (Fig. 4a) increased after surgery (Fig. 4b) according to the change in cup size.

Correlations between the change in IOP (%) and changes in BMO-MRW and c-RNFLT are shown in Table 3. The changes in BMO-MRW in the global (whole disc; r= −0.444, p=0.012), temporal (r= −0.700, $p<0.001$), and temporal superior (r= −0.482, p=0.007) segments correlated significantly with the reduction in IOP. The change in the global and temporal superior segments of the BMO-MRW correlated significantly with the change in cup size (global segment, r= −0.387, p=0.032; temporal superior segment, r = −0.432, p=0.015). Change in the global segment or other segments of the c-RNFLT did not correlate significantly

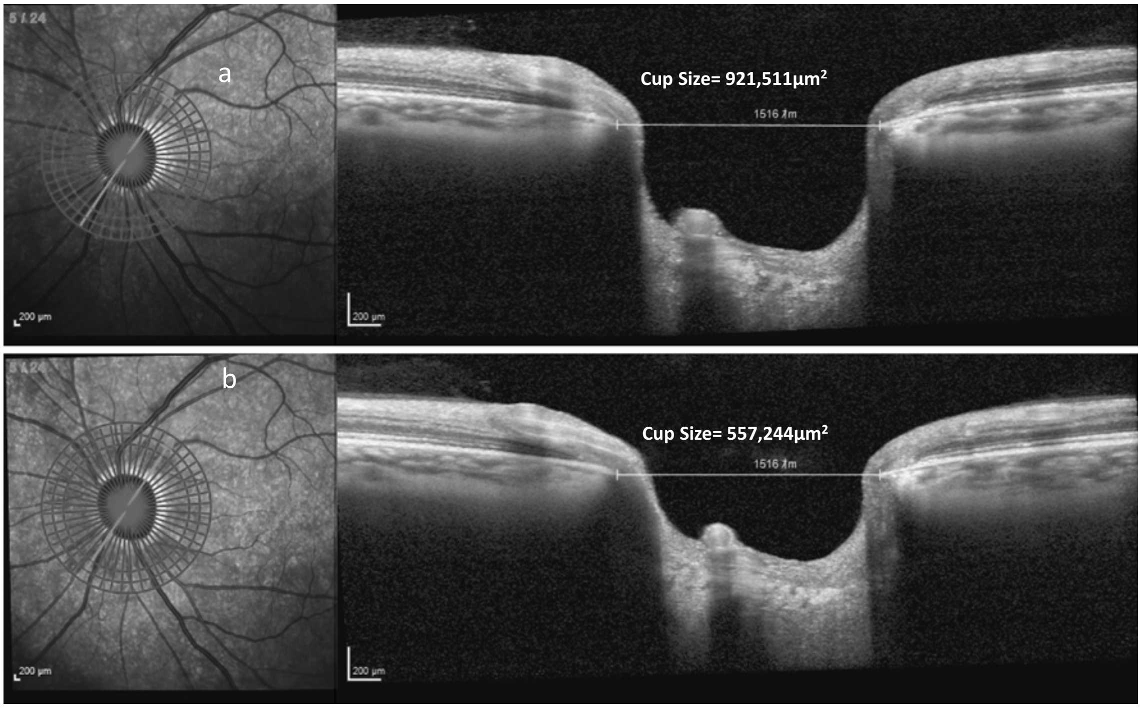

Fig. 3 A representative image of a change in cup size in a glaucomatous eye. The cup profile before surgery (921,511 μm²) (a) was markedly reduced three months after surgery (557,244 μm²) (b). This change seems to be mainly due to anterior displacement of the bottom of the cup.

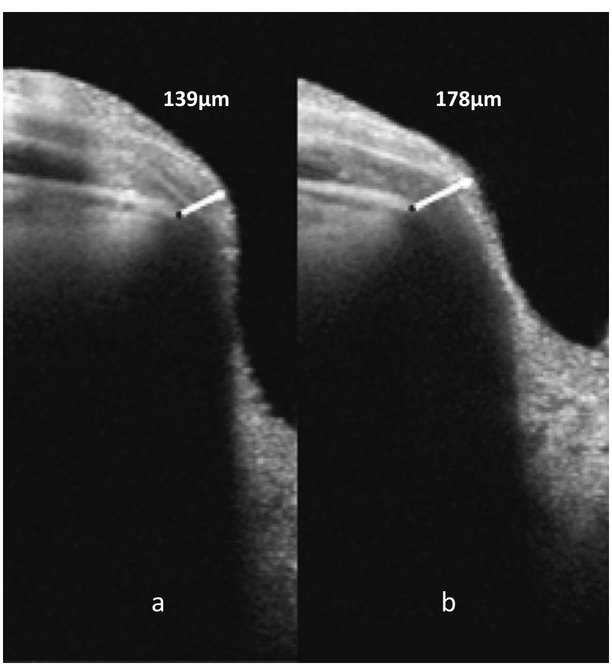

Fig. 4 A representative image of a change in BMO-MRW in a glaucomatous eye. The BMO-MRW (light blue line) before surgery (139 μm) (a) was increased three months after surgery (178 μm) (b). BMO-MRW, Bruch's membrane opening-minimum rim width.

with the change in cup size.

Stepwise multiple regression analysis was applied to analyze the correlation of changes in the global BMO-MRW (Table 4) and global c-RNFLT (Table 5) with those factors demonstrating a correlation with $p<0.2$ in univariate analysis. BMO-MRW correlated ($p<0.2$) with baseline IOP (mmHg), percent reduction in IOP, spherical equivalent (D), baseline MD (dB), baseline axial length (mm), percent change in axial length, baseline BMO area (μm²), baseline c-RNFLT (μm), and percent change in cup size. Among these factors, percent changes in axial length ($\beta= -0.33$, $p=0.034$) and cup size ($\beta= -0.50$, $p=0.002$) were statistically significant contributors to the change in BMO-MRW (Table 4). The c-RNFLT correlated ($p<0.2$) with the baseline c-RNFLT (μm), percent change in c-RNFLT, baseline MD (dB), baseline cup size (μm²), and percent change in cup size. The baseline MD ($\beta= -0.55$, p-0.002), base line cup size ($\beta= -0.36$, $p=0.031$) and percent change in cup size ($\beta=0.36$, $p=0.031$) were statistically significant contributors to the change in c-RNFLT. This finding indicated that a thinner baseline c-RNFLT increased more after surgery (Table 5).

Differences in percent changes in factors before and after surgery between subgroups were analyzed. The

Table 3 Correlations between IOP reduction (%) and BMO-MRW change (%) and c-RNFLT change (%)

	BMO-MRW		c-RNFLT	
	r	P value	r	P value
Global	−0.444	**0.012**	−0.049	0.794
Temporal	−0.700	**<0.001**	−0.217	0.224
Temporal Superior	−0.482	**0.007**	−0.266	0.334
Temporal Inferior	0.053	0.722	−0.100	0.834
Nasal	−0.080	0.723	0.254	0.707
Nasal Superior	−0.127	0.187	−0.145	0.789
Nasal Inferior	−0.426	0.063	0.315	0.465

BMO-MRW: Bruch's membrane opening minimum rim width, c-RNFLT: Circumpapillary retinal nerve fiber layer thickness, r: Spearman's rank correlation coefficient.
Statistically significant coefficients ($P<0.05$) are indicated in bold.

Table 4 Multiple regression analysis for BMO-MRW G change (%).

	Slope	SE	β	95% CI	P value
Cup size change (%)	−0.247	0.07	−0.50	−0.40, −0.01	**0.002**
Axial length change (%)	−9.783	4.40	−0.33	−18.79, −0.78	**0.034**

BMO-MRW G: Bruch's membrane opening minimum rim width global, SE: standard error, β: standard partial regression coefficient, CI: confidence interval.
The statistically significant factor ($P<0.05$) is indicated in bold.

Table 5 Multiple regression analysis for c-RNFLT G change (%).

	Slope	SE	β	95% CI	P value
Baseline MD (dB)	−0.54	0.16	−0.55	−0.86, −0.21	**0.002**
Cup size change (%)	0.13	0.06	0.36	0.01, 0.25	**0.031**
Baseline cup size (μm^2)	−8.22	0.00	−0.36	0.00, 0.00	**0.031**

MD: Mean deviation, SE: standard error, β: standard partial regression coefficient, CI: confidence interval.
The statistically significant factor ($P<0.05$) is indicated in bold.

changes in BMO area and cup size were significantly greater in female subjects (Table 6) and changes in BMO-MRW in the global and nasal-inferior segments were greater in patients aged <65 years than in those aged ≥ 65 years (Table 7). Changes in c-RNFL in the temporal-inferior segments showed a greater increase in eyes with an MD ≤ −14.7 dB (the average MD) than in those with an MD > −14.7 dB (Table 8). However, there were no significant differences in percent changes in factors between the subtypes of open-angle glaucoma (Table 9).

Discussion

In this study, we investigated the relationship between cup reversal and the structure of the ONH using SD-OCT-derived BMO-MRW and c-RNFLT measurements in eyes with open-angle glaucoma that achieved at least a 20% IOP reduction after TLE. The degree of cup reversal was evaluated by measuring the area demarcated by a line joining the BMO of the cup profile and the pre-laminar tissue surface in both preoperative and postoperative images. BMO-MRW increased significantly, and the cup size decreased significantly after surgery. Changes in the global, temporal, and temporal superior segments of the BMO-MRW correlated significantly with the change in IOP. In multiple regression analysis, the percent changes in cup size and axial length, but not the change in IOP, were more closely related to the change in BMO-MRW. In contrast, although there was no significant increase in c-

Table 6 Differences in percent changes of factors between genders.

(%)	Male (n = 13)	Female (n = 18)	P value
IOP reduction	− 43.2 ± 9.4	− 42.9 ± 18.4	0.471
Axial length change	− 0.4 ± 0.2	− 0.3 ± 0.4	0.215
BMO Area change	1.1 ± 2.2	− 4.1 ± 10.4	**0.008**
BMO-MRW change			
Global	4.8 ± 7.8	8.7 ± 10.4	0.215
Temporal	5.3 ± 7.0	10.7 ± 30.6	0.810
Temporal Superior	8.2 ± 21.7	10.7 ± 22.9	0.280
Temporal Inferior	7.4 ± 17.0	10.2 ± 19.0	0.401
Nasal	3.7 ± 13.1	13.5 ± 21.6	0.150
Nasal Superior	13.0 ± 26.7	8.4 ± 12.3	0.873
Nasal Inferior	4.4 ± 12.3	7.7 ± 20.7	0.230
c-RNFLT change			
Global	4.7 ± 7.7	0.6 ± 6.0	0.118
Temporal	5.6 ± 13.8	1.0 ± 8.7	0.246
Temporal Superior	5.0 ± 13.2	1.0 ± 6.7	0.660
Temporal Inferior	7.9 ± 11.4	0.2 ± 8.3	0.104
Nasal	2.2 ± 5.0	0.3 ± 10.7	0.280
Nasal Superior	6.2 ± 12.4	1.0 ± 7.3	0.230
Nasal Inferior	6.5 ± 10.8	− 0.5 ± 7.3	0.203
Cup Size change	− 6.9 ± 11.6	− 19.1 ± 22.0	**0.031**

Continuous variables are expressed as mean ± SD, IOP: Intraocular pressure, BMO-Area: Bruch's membrane opening area, BMO-MRW: Bruch's membrane opening minimum rim width, c-RNFLT: Circumpapillary retinal nerve fiber layer thickness.
Statistically significant differences (P < 0.05) by Mann-Whitney *U*-test are indicated in bold.

RNFLT following surgery, the baseline MD, cup size at baseline, and percent change in cup size were statistically significant contributors to the change in c-RNFLT.

There are several reports of changes in the structure of the ONH after treatment for glaucoma[1-6]. Gietzelt et al.[13] investigated changes in BMO-based parameters and RNFLT and found that global and sectoral BMO-MRW and BMO-minimum rim area measurements increased significantly for at least one year after TLE. However, the physiologic bases of the changes in BMO-MRW and c-RNFLT and their correlation with the change in cup size and reduction of IOP remained unclear. Given that BMO-MRW is considered by the measurement algorithm to be equivalent to RNFLT at the edge of the ONH, it is important to clarify the differences in changes between BMO-MRW and c-RNFLT caused by reduction of IOP and the reasons for these differences.

Lee et al.[15] reported a reversal of displacement of the lamina cribrosa, and Yoshikawa et al.[16] reported a decrease in the depth of the lamina cribrosa and shortening of the axial length after surgery for glaucoma, in which reduction of IOP resulted in reversal of cup size. Therefore, reversal of cup size can be considered to result from forward movement of the lamina cribrosa. This may explain the thickening of the BMO-MRW after reduction of IOP. Why does displacement of the lamina cribrosa cause a change in the BMO-MRW? One explanation is that, under high IOP, retinal nerve fibers running inside the ONH are stretched toward the bottom of the cup because the lamina cribrosa is displaced backward, and with forward movement of the lamina cribrosa after reduction of IOP, the stretched retinal nerve fibers return to their original position or slide back distally.[17] This may have resulted in the thickening of the BMO-MRW after the reduction of cup size. Furthermore, retinal blood vessels with large diameters are densely packed in the peripapillary area. Therefore, as with retinal nerve fibers, the stretching of these blood vessels toward the bottom of the cup may also be influenced by the forward movement of the lamina cribrosa after reduction of IOP. Considering that the response of blood vessels in terms of expansion and contraction seems to be stronger than that of nerve fibers, retinal

Table 7 Differences in percent changes of factors between those with age <65 and ≥65.

(%)	Age<65 (n=9)	Age≥65 (n=22)	P value
IOP reduction	−36.1±12.8	−45.8±15.3	0.074
Axial length change	−0.2±0.3	−0.4±0.3	0.117
BMO Area change	−5.3±13.5	−0.6±4.9	0.098
BMO-MRW change			
Global	2.0±6.1	9.1±9.9	**0.024**
Temporal	1.5±15.9	11.3±25.8	0.151
Temporal Superior	5.2±13.5	11.5±24.8	1.000
Temporal Inferior	4.0±11.0	11.1±20.0	0.459
Nasal	3.6±12.0	11.7±20.8	0.361
Nasal Superior	−1.5±7.0	15.2±20.8	**0.001**
Nasal Inferior	3.3±8.9	7.5±20.0	0.486
c-RNFLT change			
Global	0.3±6.9	3.2±6.9	0.432
Temporal	1.0±16.5	3.7±8.5	0.117
Temporal Superior	−0.6±7.0	4.0±10.8	0.164
Temporal Inferior	0.8±10.6	4.5±10.2	0.601
Nasal	1.8±7.3	0.9±9.3	0.744
Nasal Superior	1.2±6.1	4.0±11.1	0.338
Nasal Inferior	−0.2±7.8	3.5±10.0	0.130
Cup Size change	−10.0±14.3	−15.6±20.9	0.794

Continuous variables are expressed as mean±SD, IOP: Intraocular pressure, BMO-Area: Bruch's membrane opening area, BMO-MRW: Bruch's membrane opening minimum rim width, c-RNFLT: Circum-papillary retinal nerve fiber layer thickness.
Statistically significant differences (P<0.05) by Mann-Whitney *U*-test are indicated in bold.

blood vessels in the peripapillary area may also have a role in thickening of the BMO-MRW after reduction of cup size.

Several studies have reported conflicting results regarding the changes in RNFLT evaluated by OCT after changes in c-RNFLT.[18–21] Aydin et al.[18] found a significant TLE-related increase in the overall mean RNFLT, ranging from −12.7 μm to 36.5 μm (median 9.9 μm). They also showed that the increase in mean RNFLT correlated significantly with the extent of IOP reduction (0.5 μm/mmHg). In contrast, Raghu et al.[21] reported a temporary increase in RNFLT at one week after TLE; however, the values reverted within three months. Other studies found no significant changes in the RNFLT overall.[13, 19, 20] In our study, there was no significant increase in the RNFLT except for the temporal-inferior segment. However, the percent change in RNFLT did not correlate significantly with the reduction in IOP. Multivariate analysis indicated that the MD and cup size at baseline and the percent change in cup size were statistically significant contributors to the change in c-RNFLT. However, this meant that eyes with a worse MD and smaller cup size at baseline and less change in cup size showed a greater increase in c-RNFLT. Therefore, in contrast with BMO-MRW, changes in c-RNFLT after reduction of IOP seem to be independent of a reduction in cup size or a change in IOP. The exact reason for the changes in c-RNFLT is unclear but may be related to unknown structural factors that are influenced by reduction of IOP. Further studies are needed to clarify the discrepancy between changes in BMO-MRW and those in c-RNFLT after reduction of IOP.

According to our findings, BMO-MRW, which represents RNFLT at the edge of the optic disc, seems to be a parameter sensitive to increasing optic disc cupping because the retinal nerve fibers at the disc edge can be stretched toward the bottom of the cup with increasing cupping and thinning and vice versa. On the other hand, c-RNFLT is the thickness measured 3.5 mm from the center of the BMO. Therefore, c-RNFLT seems to be less influenced by structural changes in the optic disc cup induced by fluctuation of IOP and may be more suitable for evalu-

Table 8 Differences in percent changes of factors between those with MD＞−14.7 dB and MD≦−14.7 dB.

(%)	MD＞−14.7 dB (n = 15)	MD≦−14.7 dB (n = 16)	P value
IOP reduction	−40.3 ± 13.1	−45.6 ± 16.7	0.260
Axial length change	−0.3 ± 0.3	−0.3 ± 0.3	0.968
BMO Area change	−3.8 ± 11.7	−0.2 ± 2.5	0.782
BMO-MRW change			
Global	5.3 ± 6.9	8.7 ± 11.4	0.406
Temporal	1.0 ± 17.9	15.5 ± 26.5	0.385
Temporal Superior	6.3 ± 12.1	12.9 ± 28.6	0.843
Temporal Inferior	3.9 ± 15.4	13.8 ± 19.3	0.236
Nasal	12.1 ± 20.0	6.8 ± 18.0	0.580
Nasal Superior	4.5 ± 9.6	15.8 ± 24.5	0.206
Nasal Inferior	5.5 ± 21.3	7.0 ± 13.7	0.813
c-RNFLT change			
Global	−0.3 ± 5.0	4.8 ± 7.8	0.085
Temporal	−1.9 ± 8.4	7.5 ± 11.7	0.055
Temporal Superior	−0.4 ± 5.3	5.5 ± 12.4	0.069
Temporal Inferior	−2.5 ± 7.2	9.0 ± 9.7	**0.001**
Nasal	−0.3 ± 8.1	2.5 ± 9.3	0.527
Nasal Superior	−0.3 ± 3.1	6.4 ± 12.9	0.075
Nasal Inferior	1.7 ± 3.1	3.0 ± 10.9	0.414
Cup Size change	−11.7 ± 14.3	−17.0 ± 22.7	0.607

Continuous variables are expressed as mean ± SD, IOP: Intraocular pressure, MD: Mean deviation, BMO-Area: Bruch's membrane opening area, BMO-MRW: Bruch's membrane opening minimum rim width, c-RNFLT: Circum-papillary retinal nerve fiber layer thickness.
Statistically significant differences (P＜0.05) by Mann-Whitney *U*-test are indicated in bold.

ating the true relationship with the functional damage of glaucoma. However, c-RNFLT may still be influenced by fluctuations in IOP, particularly in eyes with advanced glaucoma. These findings should be taken into account when evaluating the structure-function relationship in glaucoma.

In this study, the decreases in BMO area and cup size was greater in female subjects than in male subjects, despite a lack of difference in percent reduction of IOP. This was another interesting finding and indicates that there may be a fundamental, sex-related difference in the structure of the optic nerve head. The reason for the greater decrease in BMO-MRW in older patients is not clear. One reason may be that older patients (those aged ≧65 years) showed a slightly greater reduction in IOP. The stage of the disease may also contribute to changes in structure. In our study, the c-RNFL in the temporal-inferior segments showed a greater increase in patients with an MD ≤ −14.7 db. However, this means that patients with a worse MD showed a greater increase in c-RNFLT. Like age, the difference in the reduction of IOP between patients with an MD ＞ −14.7 dB and MD ≤ −14.7 dB may have been a reason in part.

Our study has several limitations. First, the number of eyes evaluated was relatively small. Second, we only evaluated changes in the BMO-MRW before and three months after surgery. Therefore, the time course of the changes after surgery is unclear. We intended to evaluate the structural changes after reversal of cupping in as much detail as possible. In the early phase after surgery, postoperative inflammation or tissue edema due to low pressure may influence the structure, and long after surgery, progression of glaucoma itself may alter the results. Therefore, we timed the evaluation for three months after surgery. Third, we measured cup size in two radial scans only, one passing from temporal-superior to nasal-inferior and the other from temporal-inferior to nasal-superior. Although there is no established method for measuring cup size with SD-OCT and the two scans cannot express all changes in cup volume, the temporal-superior and

Table 9 Differences in percent changes of factors between subtypes of open-angle glaucoma.

(%)	NTG (n = 6)	POAG (n = 21)	XFG (n = 4)	P value
IOP reduction	− 32.3 ± 9.3	− 44.7 ± 14.2	− 50.2 ± 21.3	0.144
Axial length change	− 0.2 ± 0.2	− 0.3 ± 0.3	− 0.5 ± 0.4	0.374
BMO Area change	− 6.3 ± 17.1	− 1.4 ± 4.7	1.6 ± 2.9	0.309
BMO-MRW change				
Global	4.1 ± 2.0	6.5 ± 9.4	14.4 ± 14.3	0.604
Temporal	− 3.8 ± 12.6	10.9 ± 26.7	14.0 ± 12.3	0.090
Temporal Superior	8.3 ± 4.8	4.1 ± 12.5	41.2 ± 47.3	0.573
Temporal Inferior	10.5 ± 18.3	8.0 ± 18.0	11.8 ± 21.6	0.978
Nasal	9.2 ± 5.5	8.9 ± 21.9	12.2 ± 17.7	0.657
Nasal Superior	3.5 ± 13.5	8.7 ± 10.2	29.5 ± 46.5	0.471
Nasal Inferior	4.0 ± 6.9	7.0 ± 20.6	6.0 ± 11.7	0.954
c-RNFLT change				
Global	5.2 ± 10.6	1.6 ± 5.9	1.9 ± 6.5	0.954
Temporal	3.9 ± 8.0	2.8 ± 12.8	2.1 ± 6.4	0.923
Temporal Superior	4.2 ± 19.6	2.6 ± 6.1	0.5 ± 9.1	0.393
Temporal Inferior	2.2 ± 7.3	1.8 ± 8.8	14.2 ± 16.4	0.488
Nasal	4.9 ± 10.7	0.3 ± 8.8	− 0.4 ± 3.0	0.497
Nasal Superior	6.9 ± 15.3	3.1 ± 6.8	− 2.0 ± 15.2	0.431
Nasal Inferior	7.1 ± 12.3	1.8 ± 7.7	− 1.3 ± 13.2	0.710
Cup Size change	− 6.5 ± 7.0	− 11.8 ± 15.2	− 36.4 ± 35.1	0.173

Continuous variables are expressed as mean ± SD, NTG: Normal tension glaucoma, POAG: Primary open angle glaucoma, XFG: Exfoliation glaucoma, IOP: Intraocular pressure, BMO-Area: Bruch's membrane opening area, BMO-MRW: Bruch's membrane opening minimum rim width, c-RNFLT: Circum-papillary retinal nerve fiber layer thickness.

temporal-inferior portions of the optic disc are usually the locations most damaged in glaucoma. Therefore, we believe that the two scan lines containing the temporal (superior and inferior) segments were appropriate for this study.

In conclusion, we confirmed that BMO-MRW increased when the IOP was sufficiently reduced (by >20%). However, the changes in BMO-MRW correlated with change in the cup size rather than with change in the IOP. Furthermore, the changes in BMO-MRW did not correlate with the changes in c-RNFLT. The increase in BMO-MRW after reduction of IOP seemed to represent the return of the retinal nerve fibers that had stretched toward the bottom of the cup with displacement of the lamina cribrosa during high IOP to their original position.

Acknowledgements: This research was supported by JSPS KAKENHI (Grant Number JP17K11436).

Conflicts of interest: Goji Tomita has received unlimited research funding from Santen Pharmaceutical, Senju Pharmaceutical, and Eisai Pharmaceutical. Otherwise, the authors declare no conflicts of interest.

References

1) Quigley HA. Childhood glaucoma: results with trabeculotomy and study of reversible cupping. Ophthalmology. 1989; 3: 219-26.
2) Raghu N, Pandav SS, Kaushik S, Ichhpujani P, Gupta A. Effect of trabeculectomy on RNFL thickness and optic disc parameters using optical coherence tomography. Eye. 2012; 26: 1131-7.
3) Topouzis F, Peng F, Kotas-Neumann R, Garcia R, Sanguinet J, Yu F, et al. Longitudinal changes in optic disc topography of adult patients after trabeculectomy. Ophthalmology. 1999; 106: 1147-51.
4) Bowd C, Weinreb RN, Lee B, Emdadi A, Zangwill LM. Optic disk topography after medical treatment to reduce intraocular pressure. Am J Ophthalmol. 2000; 130: 280-6.
5) Lesk MR, Spaeth GL, Azuara-Blanco A, Araujo SV, Katz LJ, Terebuh AK, et al. Reversal of optic disc cupping after glaucoma surgery analyzed with a scanning laser tomograph. Ophthalmology. 1999; 106: 1013-8.
6) Irak I, Zangwill L, Garden V, Shakiba S, Weinreb RN. Change in optic disk topography after trabeculectomy. Am J Ophthalmol. 1996; 122: 690-5.
7) Park KH, Kim DM, Youn DH. Short-term change of optic nerve head topography after trabeculectomy in adult glaucoma pa-

tients as measured by Heidelberg retina tomograph. Korean J Ophthalmol. 1997; 11: 1-6.
8) Kotecha A, Siriwardena D, Fitzke FW, Hitchings RA, Khaw PT. Optic disc changes following trabeculectomy longitudinal and localisation of change. Br J Ophthalmol. 2001; 85: 956-61.
9) Lee EJ, Kim TW. Reversal of lamina cribrosa displacement and thickness after trabeculectomy in glaucoma. Ophthalmology. 2012; 119: 1359-66.
10) Reis AS, Sharpe GP, Yang H, Nicolela MT, Burgoyne CF, Chauhan BC. Optic disc margin anatomy in patients with glaucoma and normal controls with spectral domain optical coherence tomography. Ophthalmology. 2012; 119: 738-47.
11) Gardiner SK, Ren R, Yang H, Fortune B, Burgoyne CF, Demirel S. A method to estimate the amount of neuroretinal rim tissue in glaucoma: comparison with current methods for measuring rim area. Am J Ophthalmol. 2014; 157: 540-9.
12) Chauhan BC, O'Leary N, Almobarak FA, Reis ASC, Yang H, Sharpe GP, et al. Enhanced detection of open-angle glaucoma with an anatomically accurate optical coherence tomography-derived neuroretinal rim parameter. Ophthalmology. 2013; 120: 535-43.
13) Gietzelt C, Lemke J, Schaub F, Hermann MM, Dietlein TS, Cursiefen C, et al. Structural reversal of disc cupping after trabeculectomy alters Bruch membrane opening-based parameters to assess neuroretinal rim. Am J Ophthalmol. 2018; 194: 143-52.
14) Reis AS, O'Leary N, Yang H, Sharpe GP, Nicolela MT, Burgoyne CF, et al. Influence of clinically invisible, but optical coherence tomography detected, optic disc margin anatomy on neuroretinal rim evaluation. Invest Ophthalmol Vis Sci. 2012; 53: 1852-60.
15) Fleiss JL. The Design and Analysis of Clinical Experiments. New York, NY: John Wiley & Sons; 1986. p. 1-32.
16) Lee EJ, Kim TW. Reversal of lamina cribrosa displacement and thickness after trabeculectomy in glaucoma. Ophthalmology. 2012; 119: 1359-66.
17) Yoshikawa M, Akagi T, Hangai M, Ohashi-Ikeda H, Takayama K, Morooka S, et al. Alterations in the neural and connective tissue components of glaucomatous cupping after glaucoma surgery using swept-source optical coherence tomography. Invest Ophthalmol Vis Sci. 2014; 55: 477-84.
18) Takagi S, Tomita G. Changes in the thickness of the macular ganglion cell complex and retinal nerve fiber layer over time after surgery in a case of juvenile glaucoma. Am J Ophthalmol Case Rep. 2016; 2: 41-3.
19) Aydin A, Wollstein G, Price LL, Fujimoto JG, Schuman JS. Changes in the thickness of the macular ganglion cell complex and retinal nerve fiber layer over time after surgery in a case of juvenile glaucoma. Ophthalmology. 2003; 110: 1506-11.
20) Chang PT, Sekhon N, Budenz DL, Feuer WJ, Park PW, Anderson DR. Effect of lowering intraocular pressure on optical coherence tomography measurement of peripapillary retinal nerve fiber layer thickness. Ophthalmology. 2007; 114: 2252-8.
21) Rebolleda G, Muñoz-Negrete FJ, Noval S. Evaluation of changes in peripapillary nerve fiber layer thickness after deep sclerectomy with optical coherence tomography. Ophthalmology. 2007; 114: 488-93.
22) Raghu N, Pandav SS, Kaushik S, Ichhpujani P, Gupta A. Effect of trabeculectomy on RNFL thickness and optic disc parameters using optical coherence tomography. Eye. 2012; 26: 1131-7.